Journal of Alloys and Compounds 533 (2012) 88–92

Contents lists available at SciVerse ScienceDirect

Journal of Alloys and Compounds

journal homepage: www.elsevier.com/locate/jallcom

Synthesis and field-emission properties of novel hierarchical ZnO hexagonal towers

Ping Wang [a], Xitian Zhang [a,*], Jing Wen [a], LiLi Wu [a], Hong Gao [a], E. Zhang [a,*], Guoqing Miao [b]

[a] Key Laboratory of Photoelectric Bandgap Materials, Ministry of Education, School of Physics and Electronic Engineering, Harbin Normal University, Harbin 150025, People's Republic of China

[b] Key Laboratory of Excited State Processes, Changchun Institute of Optics, Fine Mechanics and Physics, Chinese Academy of Sciences, 16-East South Lake Road, Changchun 130021, People's Republic of China

ARTICLE INFO

Article history:
Received 10 February 2012
Received in revised form 20 March 2012
Accepted 1 April 2012
Available online 11 April 2012

Keywords:
Field-emission properties
Hierarchical ZnO hexagonal towers
Layer structure

ABSTRACT

Novel hierarchical ZnO hexagonal towers were fabricated via chemical vapor deposition for the first time by adding trace Fe power in the precursor as a catalyst. The scanning electron microscopy images showed that the outside surface of novel hierarchical ZnO hexagonal towers was layer-by-layer assembly. X-ray diffraction pattern indicated that the hierarchical ZnO hexagonal towers grew preferentially along the [0 0 0 1] direction. Intense UV emission centered at 380 nm was observed at room temperature. Moreover, their field-emission properties were studied. A low turn-on electric field of 2.37 V μm^{-1} and high field enhancement factor of about 2691 were obtained, due to the novel layer structure and high crystalline quality. This kind of hierarchical ZnO microstructures could be a good candidate for high performance field emission devices.

1. Introduction

Recently, research on field-emission (FE) properties of one-dimensional nanostructures has attracted a great deal of attention due to growing demand for vacuum microwave amplifiers, flat-panel displays and X-ray sources, etc. [1]. For these commercial applications, how to improve the FE performance has become a challenge issue. Generally, there are two effective ways to meet the challenge. One is optimizing the geometric factor by increasing the alignment of the nanostructures; the other is increasing conductivity and reducing the work function by selective element doping [2]. On the other hand, the field enhancement factor β is a very important parameter for appraising the performances of FE, and it relates to the structure, shape, size, crystalline, aspect ratio, etc. [3]. Many reports were focused on the development of nanostructures with different morphology or shape, such as ZnS branched architectures [4], hierarchical single-crystalline β-SiC nanoarchitectures [5], ZnS tetrapod tree-like heterostructures [6], carbon-in-Al_4C_3 nanowires [7] and sixfold-symmetrical hierarchical ZnO [8].

ZnO, a very important multifunctional n-type semiconductor, is usually used to fabricate FE devices, ultraviolet photodetectors, and light emitting diodes. Focus more on FE properties from ZnO has been increasing due to a wide range of morphologies and its chemical stability good enough. Many studies have already been performed regarding the synthesis and FE characteristics of ZnO nanostructures [8–13], concluding that one-dimensional hierarchical structure is one of the ideal morphologies for achieving high FE current density at a low electric field [11]. However, understanding of hierarchical ZnO micro-/nano-structures and their associated FE properties is limited, although such problem is very important to their potential applications.

In this paper, novel hierarchical ZnO hexagonal towers (NHZOHTs) are designed and successfully synthesized based on the above information gathered. The growth mechanism is proposed in terms of the symmetry of crystalline structure and the morphological evolution of the as-synthesized NHZOHTs. Their photoluminescence (PL) and FE properties are measured, respectively. The low turn-on electric field of 2.37 V μm^{-1} and the high field enhancement factor of about 2691 from the as-synthesized NHZOHTs indicate that such unique morphology of ZnO should be valuable for the optimization of field emitters.

2. Experimental details

The NHZOHTs were carried out by a chemical vapor deposition process. The mixture of ZnO powder and trace amounts of Fe power as catalyst was loaded into one end of an alumina boat. Si wafers sputtered with Au were placed at the downstream of the precursor. The boat was placed inside an alumina tube that was inserted into a horizontal furnace. The furnace was heated to a preset temperature (1300 °C) and maintained at this temperature for 30 min. Pure N_2 as carrier gas flows into the alumina tube at a flow rate of 100 sccm and a pressure of 500 Pa. Finally, the system was naturally cooled down to the ambient temperature.

* Corresponding authors.
E-mail addresses: xtzhangzhang@hotmail.com (X.T.Zhang), hsdzhe@126.com (E. Zhang).

0925-8388/$ – see front matter © 2012 Elsevier B.V. All rights reserved.
http://dx.doi.org/10.1016/j.jallcom.2012.04.003

The morphology and chemical composition of the as-prepared NHZOHTs were characterized by field-emission scanning electron microscopy (FE-SEM; S-4800, Hitachi, Japan), equipped with energy dispersive X-ray spectrometer. The crystal structure of the NHZOHTs was characterized by X-ray powder diffraction (XRD, D8 advance, Brook, Germany). PL spectrum was measured using a micro-Raman spectrometer (J-Y, HR800, France), employing the 325 nm line of a He–Cd laser as the excitation light source, and Raman spectra were recorded with the laser at a wavelength of 488 nm. All these measurements were made at room temperature.

3. Results and discussion

SEM is employed to depict the surface morphology of the sample. Fig. 1(a) shows low-magnification morphology of the products and they have tower-like shapes. Layer structures are discernible on the surface of the hexagonal towers, as shown in Fig. 1(b), which length is tens of micrometers. Each NHZOHT has a hexagonal cross-section consistent with the symmetry characteristic of ZnO (0 0 0 1) facet, indicating that it grows along the ⟨0 0 0 1⟩ direction or *c*-axis. In addition, the NHZOHTs have a slightly tapering structure along the *c*-axis. From the observation of the hexagonal cross-section, the tower is composed of two hexagonal columns, and one rotates 30° in its own plane about the *c*-axis. Layer-by-layer structures were clearly visible, as shown in the inset of Fig. 1(b). The diagonal length of their hexagonal cross-section for the bases is about 1.5 μm and the thickness of each layer is about 30 nm. The NHZOHTs are obviously different from the reported one-dimensional nanostructure [14]. In order to measure the chemical composition of the NHZOHTs, EDX spectrum is performed on the individual NHZOHT, as shown in Fig. 1(c), indicating that the NHZOHTs only contain elements Zn and O, although Fe existed in the precursor.

Fig. 2 shows an XRD pattern of the as-synthesized NHZOHTs. All diffraction peaks in this pattern can be indexed to the hexagonal wurtzite structure ZnO (JCPDS Card No. 80-0075), indicating that the NHZOHTs grow preferentially along the ⟨0 0 0 1⟩ direction. No peaks of other phases can be detected within the limit of the equipment. Furthermore, the further structural information of the sample was investigated employing the Raman method [15] (Fig. 3). The peaks at about 98, 331, 436, and 585 cm^{-1} correspond to the E_{2L}, E_{2H}–E_{2L}, E_{2H} and E_{1L} phonon modes of the ZnO modes, respectively. The peaks located at 203 and 659 cm^{-1} are assigned to the multi-phonon processes. According to XRD result and Raman spectra, we believe that the as-synthesized NHZOHTs are pure ZnO phase.

What exactly happened to cause so complicated structure formed? To shed light on the underlying growth mechanism of this novel structure, a series of experiments were conducted: (i) ZnO nanowires with a uniform diameter were synthesized under the same growth conditions, except no Fe in precursor, as shown in Fig. 1(d); (ii) Fig. 4(a) shows a scenario image found at the lower temperature growth area near by NHZOHTs; (iii) there is no alloy tip to be observed on the top of NHZOHTs (Fig. 4(b)). Based on the above information gathered, conclusions are that the growth of the ZnO rods is possibly ascribed to the vapor–solid (VS) mechanism; epitaxial growth is a necessary process; the formation of NHZOHTs is likely attributed to the Fe acting as catalyst. Furthermore, the morphology evolution of Fig. 4(a) to (b) reveals that the second growth of the ZnO rod begins from the top part of rod by expitaxial mode. Hence, the formation of the NHZOHTs can be separated into two major stages. The first is a growth of the ZnO rods along the [0 0 0 1] direction by VS mechanism. The second stage is the epitaxial growth of the rods from the top part to base due to the surrounding Fe vapor as catalyst. Subsequently, the Ostwald ripening [16] processes dominate the evolution of the rods. The larger thin layers adsorb smaller thin layers, and then grow gradually into the NHZOHTs by their self-assembly, being subject to the minimum principle of the surface energy. We propose that the Stranski–Krastanow growth mode dominates the whole growth process of the NHZOHTs. On the other hand, the content of the

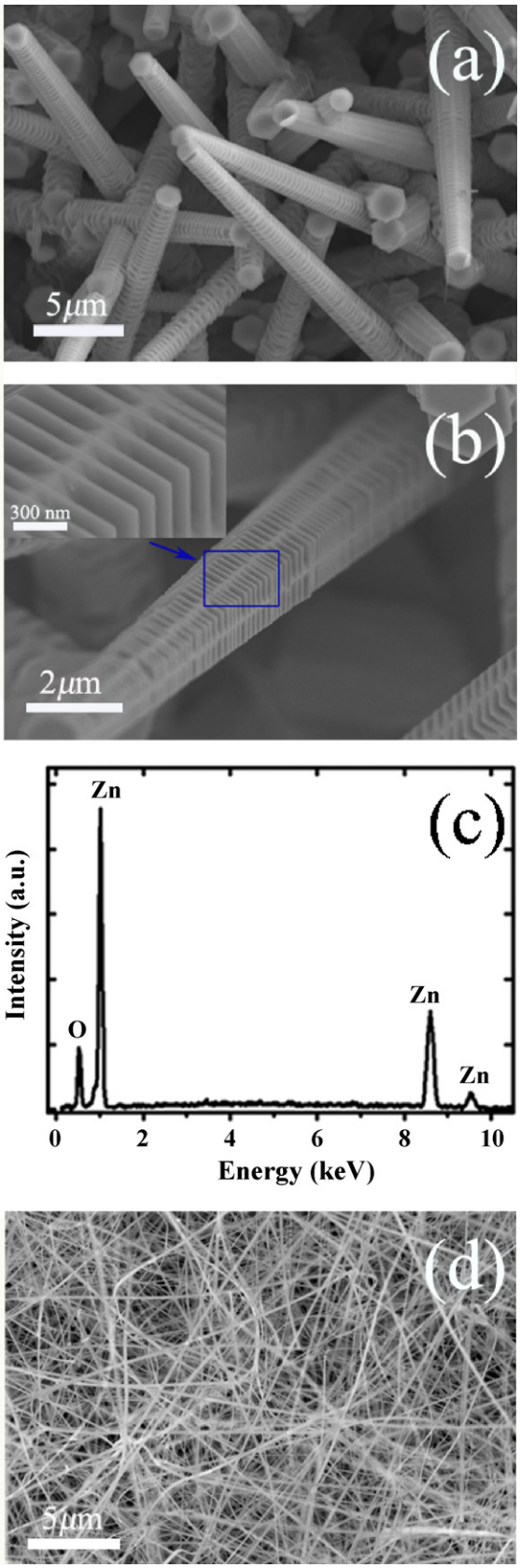

Fig. 1. (a) Typical SEM image of the as-synthesized NHZOHTs; (b) a high-magnification SEM image. The inset is the enlarged SEM image of a blue area in (b); (c) the corresponding EDX spectrum of NHZOHTs; (d) for a comparison, presenting ZnO nanowires synthesized under the same growth conditions except without Fe in the precursor. (For interpretation of the references to color in this figure legend, the reader is referred to the web version of the article.)

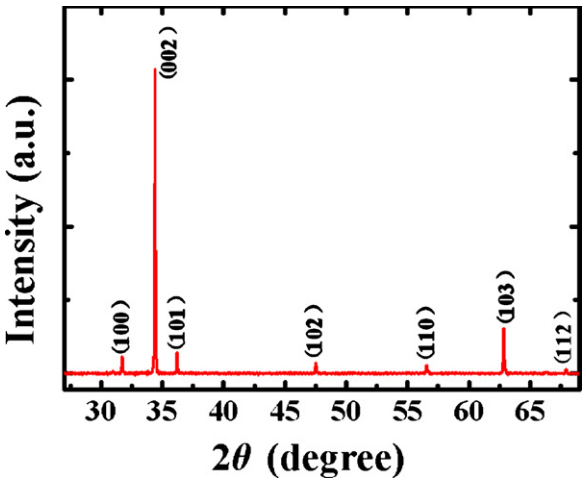

Fig. 2. XRD pattern of as-synthesized NHZOHTs.

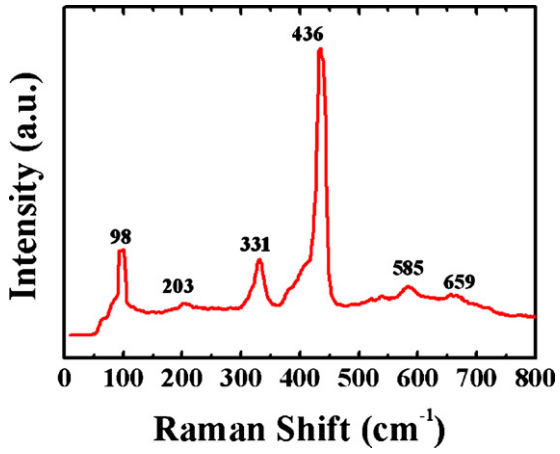

Fig. 3. Raman scattering spectrum of the NHZOHTs.

precursor plays an important role in the formation of the grown ZnO nanostructure from our experimental data. Dai et al. [17] suggested a similar opinion that the morphology and structure of products depend not only on the processing parameters adopted but also on the source materials employed.

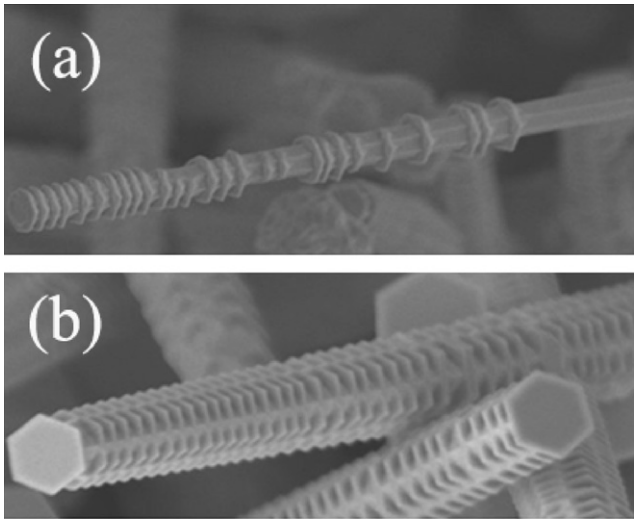

Fig. 4. (a) A mid-process of NHZOHTs and (b) a NHZOHT.

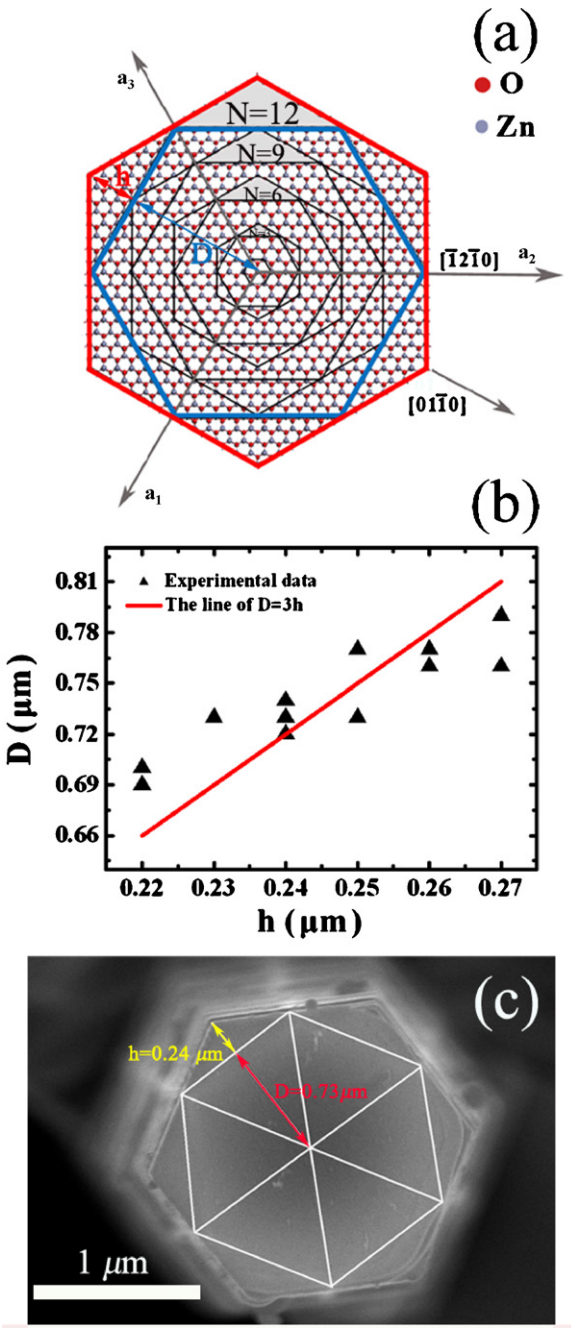

Fig. 5. (a) The atomic structure model of ZnO in (0 0 0 1); (b) D as a function of h, solid triangle (▲): experimental data. Red line for $D = 3h$; (c) a representative SEM image of a hexagonal cross-section. (For interpretation of the references to color in this figure legend, the reader is referred to the web version of the article.)

As is well known, ZnO easily forms hexagonal micro-/nanorods, which are closed by six $\{0\,1\,\bar{1}\,0\}$ crystal facets. However, as can been seen from atomic structure model (Fig. 5(a)), hexagonal rods have an opportunity to epitaxially grow along $\langle 0\,1\,\bar{1}\,0\rangle$ direction after every three growth cycle, i.e. the number of atom layers (N) satisfies $N = 3n$ ($n = 1, 2, 3, \ldots$). According to the atomic structure model and geometry calculation, $D = 3h$, where the length of diagonal line for the hexagonal cross-section formed after epitaxial growth equals the sum of $2D$ and $2h$. In the experiment, ten of hexagonal cross-section of individual NHZOHT was measured, as shown in Fig. 5(b). The maximum relative error between the experimental data and theoretical value is 6%. Considering the uncertainty of measurement, the value of D/h is 3.0 ± 0.7, and the error is within

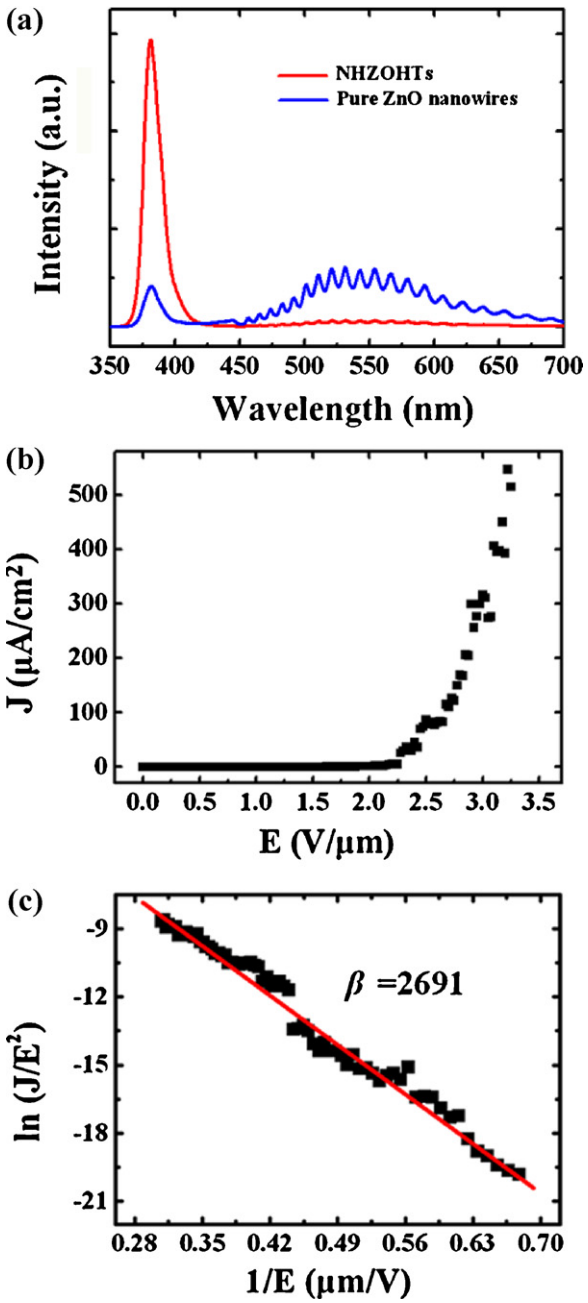

Fig. 6. (a) Room temperature PL spectra: a red curve and a blue curve are the PL spectra of the NHZOHTs and pure ZnO nanowires, respectively. The fluctuated broad band of PL spectrum is caused by micro-Raman system; (b) emission current density as a function of applied electrical field for NHZOHTs and (c) corresponding *F–N* plot. (For interpretation of the references to color in this figure legend, the reader is referred to the web version of the article.)

the allowable range. Fig. 5(c) is a representative SEM image of a hexagonal cross-section. On the other hand, the layer structure is likely attributed to the uniformly tapering of ZnO rods. Tapering results in some spaces cannot meet $N = 3n$ ($n = 1, 2, 3, \ldots$). So, these places could not further grow epitaxially. Summarizing the results, we propose that the formation of NHZOHTs contains three conditions at least: (i) the ZnO rods have a slightly tapering structure along the *c*-axis; (ii) the number of atom layers along $\langle 0\,1\,\bar{1}\,0\rangle$ direction satisfies $N = 3n$ ($n = 1, 2, 3, \ldots$); (iii) Fe has to be used as a catalyst to enhance the surface energy of $\{2\,\bar{1}\,\bar{1}\,0\}$ over $\{0\,1\,\bar{1}\,0\}$.

The PL spectroscopy is a useful method to characterize the defects and impurities in the as-synthesized products. As shown in Fig. 6(a), the PL spectrum of the NHZOHTs presents a sharp and intense peak at approximately 380 nm, which arises from the near band-edge exciton recombination, and the weak green emission is probably attributed to the low surface states and low structural defects [18]. The ratio of UV PL intensity to green PL intensity for NHZOHTs is as high as 60. The weaker green emission of NHZOHTs compared with pure ZnO nanowires, implies that NHZOHTs have higher crystal quality.

Table 1
FE data from NHZOHTs and other materials.

Materials	E_{to} (V μm^{-1})	E_{th} (V μm^{-1})	Factor β
ZnO nanoneedles [9]	2.5	4.0	
ZnO nanonails [12]	7.9		
ZnO nanotower with a small crown [10]	4.5	7.2	2100
Six-fold-symmetrical hierarchical ZnO [8]	5.6		1351
Hierarchical-structure ZnO [11]	4.8		3400
ZnO nanotubes [13]	3.5		
Hierarchical β-SiC nanoarchitectures [5]	12		
CNT [19]	3.87		1737
Carbon-in-Al_4C_3 nanowire [7]	0.65–1.3	2.3–2.6	
ZnS tetra pod tree-like heterostructures [6]	2.66		2600
MoO_3 nanowires [20]	3.5	7.65	
B nanowires [21]	5.1	11.5	
Tungsten whiskers [22]	4.0		1904
NHZOHTs	2.37		2691

Note: The turn-on field is defined as the electric field needed to obtain a current density of 10 μA/cm^2.

In order to investigate the FE properties of the NHZOHTs, the field emission *J–E* characteristic of the NHZOHTs was measured in a vacuum chamber at a low pressure ~2.0×10^{-4} Pa at room temperature. A piece of conductive glass coated with ITO thin film plays the role of an anode; the NHZOHTs were the cathode. The distance between anode–cathode was 200 μm. In the measuring circuit, emission current was directly determined. FE current density (J) as a function of applied electric field (E) for the NHZOHTs is shown in Fig. 6(b). The electron emission turn-on field of the NHZOHTs was 2.37 V μm^{-1} at the current density of 10 μA cm^{-2}. The low value of turn-on electric field surpasses those mentioned in Table 1. It suggests that the presently synthesized NHZOHTs can be used as practical field emitters.

The relationship between the current density J and the applied electric field E is further analyzed by the Fowler–Nordheim (FN) theory:

$$J = \frac{A\beta^2 E^2}{\Phi} \exp\left(-\frac{B\Phi^{3/2}}{\beta E}\right) \quad (1)$$

And Eq. (1) could be altered to:

$$\ln\left(\frac{J}{E^2}\right) = -\frac{B\Phi^{3/2}}{\beta} \times \frac{1}{E} + \ln\left(\frac{A\beta^2}{\Phi}\right) \quad (2)$$

Here, $A = 1.54 \times 10^{-6}$ A eV V^{-2}, $B = 6.83 \times 10^{3/2}$ eV$^{-3/2}$ V μm^{-1}; Φ is the work function of the emitting material (eV); β is the field enhancement factor. By plotting $\ln J/E^2$ versus $1/E$, an approximate linear relation obtained is shown in Fig. 6(c). The linearity of this curve implies the FE from these NHZOHTs is agreeing well with the FN theory. Then, the field enhancement factor can be estimated as 2691 by taking the work function of ZnO as 5.3 eV. It is known that both morphology and dimensions have a significant influence on the emitter field-enhancement factor. A little changes of the shape or the surface of the solid have a great impact on the emitted current. It is reasonable to expect a higher β for the NHZOHTs that have layer-by-layer structure. Moreover, the lattice defects in the

crystalline nanostructure could make electron migration more serious at high electronic fields. From the above PL result, the NHZOHTs only show strong emission in the UV region. The absence of a broad visible region confirms that such high crystal quality NHZOHTs are free of lattice defects, which facilitates stabilizing the emission current [4]. Considering the low turn-on field, and the high field enhancement factor of the as-synthesized NHZOHTs, it could be concluded that this structural ZnO could be a good candidate for FE devices.

4. Conclusions

In summary, NHZOHTs were successfully synthesized by a chemical vapor deposition method, using metal Fe as a catalyst. The growth mechanism for the NHZOHTs is due to second epitaxial growth of ZnO nanorods based on the atomic structure model and morphological evolution. FE measurements of the NHZOHTs show a low turn-on field of 2.37 V μm^{-1} and a high field enhancement factor of 2691 due to layer-by-layer crystallographic structure and high crystal quality, indicating that it has greatly potential applications in FE devices.

Acknowledgments

This work was partially supported by the Natural Science Foundation of China (Nos. 51172058, 61154001 and 11074060), the Key Project of Natural Science Foundation of Heilongjiang Province (ZD201112).

References

[1] X.S. Fang, Y. Bando, U.K. Gautam, C. Ye, D. Golberg, Journal of Materials Chemistry 18 (2008) 509–522.
[2] L.L. Wu, Q. Li, X.T. Zhang, T.Y. Zhai, Y.S. Bando, D. Golberg, Journal of Physical Chemistry C 115 (50) (2011) 24564–24568, http://dx.doi.org/10.1021/jp207438s.
[3] T.Y. Zhai, X.S. Fang, Y.S. Bando, Q. Liao, X.J. Xu, H.B. Zeng, Y. Ma, J.N. Yao, D. Golberg, ACS Nano 3 (2009) 949–959.
[4] Z.G. Chen, L. Cheng, H.Y. Xu, J.Z. Liu, J. Zou, T. Sekiguchi, G.Q. Lu, H.M. Cheng, Advanced Materials 22 (2010) 2376–2380.
[5] G.Z. Shen, Y. Bando, D. Golberg, Crystal Growth and Design 7 (2007) 35–38.
[6] Z.G. Chen, J. Zou, G. Liu, X.D. Yao, F. Li, X.L. Yuan, T. Sekiguchi, G.Q. Lu, H.M. Cheng, Advanced Functional Materials 18 (2008) 3063–3069.
[7] Y. Sun, H. Cui, L. Gong, J. Chen, J.C. She, Y.M. Ma, P.K. Shen, C.X. Wang, ACS Nano 5 (2011) 932–941.
[8] Z.Q. Wang, J.F. Gong, Y. Su, Y.W. Jiang, S.G. Yang, Crystal Growth and Design 10 (2010) 2455.
[9] Y.B. Li, Y. Bando, D. Golberg, Applied Physics Letters 84 (2004) 3603–3605.
[10] J. Xiao, X.X. Zhang, G.M. Zhang, Nanotechnology 19 (2008) 295706.
[11] Y.X. Liu, Y.Z. Xie, J.T. Chen, J. Liu, C.T. Gao, C. Yun, B.A. Lu, E.Q. Xie, Journal of the American Ceramic Society 94 (12) (2011) 4387–4390, http://dx.doi.org/10.1111/j.1551-2916.2011.04734.x.
[12] G.Z. Shen, Y. Bando, B.D. Liu, D. Golberg, C.J. Lee, Advanced Functional Materials 16 (2006) 410–416.
[13] R.C. Wang, C.P. Liu, J.L. Huang, S.J. Chen, Nanotechnology 17 (2006) 753–757.
[14] Y. Liang, X.T. Zhang, L. Qin, E. Zhang, H. Gao, Z.G. Zhang, Journal of Physical Chemistry B 110 (2006) 21593–21595.
[15] L. Shi, C.J. Pei, Y.M. Xu, Q. Li, Journal of the American Chemical Society 133 (2011) 10328–10331.
[16] H.Q. Lu, L.L. Wu, E. Zhang, X.T. Zhang, CrystEngComm 12 (2010) 85–88.
[17] Z.R. Dai, Z.W. Pan, Z.L. Wang, Advanced Functional Materials 13 (2003) 9–24.
[18] X.T. Zhang, Y.C. Liu, J.Y. Zhang, Y.M. Lu, D.Z. Shen, X.W. Fan, X.G. Kong, Journal of Crystal Growth 254 (2003) 80–85.
[19] D.Q. Duy, H.S. Kim, D.M. Yoon, K.J. Lee, J.W. Ha, Y.G. Hwang, C.H. Lee, B.T. Cong, Applied Surface Science 256 (2009) 1065–1068.
[20] J. Zhou, N.S. Xu, S.Z. Deng, J. Chen, J.C. She, Z.L. Wang, Advanced Materials 15 (2003) 1835–1840.
[21] F. Liu, J.F. Tian, L.H. Bao, T.Z. Yang, C.M. Shen, X.Y. Shen, Z.M. Xiao, W.G. Xie, S.Z. Deng, J. Chen, Advanced Materials 20 (2008) 2609–2615.
[22] S.L. Wang, Y.H. He, X.S. Fang, J. Zou, Y. Wang, H. Huang, P.M.F.J. Costa, M. Song, B.Y. Huang, C.T. Liu, Advanced Materials 21 (2009) 2387–2392.